iScience, Volume *25*

Supplemental information

The necroptosis-inducing pseudokinase mixed lineage kinase domain-like regulates the adipogenic differentiation of pre-adipocytes

Julie Magusto, Carine Beaupère, Marta B. Afonso, Martine Auclair, Jean-Louis Delaunay, Pierre-Antoine Soret, Gilles Courtois, Tounsia Aït-Slimane, Chantal Housset, Isabelle Jéru, Bruno Fève, Vlad Ratziu, Cecilia M.P. Rodrigues, and Jérémie Gautheron

Supplemental information

Supplementary Table 1. List of predicted off-target sequences of the CRISPR/Cas9 editing strategy, with mismatch position and genomic location, related to STAR Methods. The CRISPOR web tool (http://crispor.tefor.net/) is well recognized to predict the risk of off-target sequences by providing a cutting frequency determination (CFD) specificity score ranging from 1 to 100. The higher the number, the lower the risk of off-target effects. It is based on the accurate CFD off-target model from Doench JG et al. (Nat Biotechnol 2016 Feb;34(2):184-196), which recommends guides with a CFD specificity score > 50. The gRNA used herein to target *Mlkl* exon 1 has a CFD score of 96, *Ripk3* exon 1 a CFD score of 96 and *MLKL* exon 4 a CFD score of 86. All gRNA did not match perfectly any other genomic region. The table below provides a list of potential off-target sequences with up to three mismatches with the different gRNA used. Notably, off-targets are considered if they are flanked by an NGG motif, which corresponds to the PAM sequence allowing the Cas9 to cut DNA.

Number of mismatches	Potential off-target sequences (mismatches are in red and bold characters)	Locus of the off-target (location, gene)
	GCACACGGTTTCCTAGACGC (*Mlkl*)	
3	GCACAC**CT**T**C**TCCTAGACGC	intergenic, *Gm25904-Cpne4*
	TGGTGCGTCAGCGGTTCCTC (*Ripk3*)	
3	TGGTG**A**GTCAG**TA**GTTCCTC	intergenic, *Cntn5-Gm25365*
3	T**A**GTG**A**G**A**CAGCGGTTCCTC	intron, *Cog5*
3	TGGT**C**C**T**TCAGCGGTTCC**C**C	intergenic, *Kcnq1*
3	TGGTGCG**C**CAGC**T**GT**G**CCTC	intron, *Galnt15*
3	TGGT**T**CGTCAGCGGTTC**AG**C	exon, *Sypl*
2	TGGTG**G**GTCAGC**T**GTTCCTC	intergenic, *Gm9824-9996/Soga3*
	AGTGAGGCAGACTTTCAATA (*MLKL*)	
3	AGTGAGG**G**AG**G**C**C**TTCAATA	intergenic, *C1D*
3	AGTGA**T**G**G**AGAC**A**TTCAATA	intergenic, *IGSF9B*
3	AGTG**T**GGCAGAC**A**TT**A**AATA	intergenic, *PPAP2B*
3	AGT**T**AGG**T**AGAC**C**TTCAATA	intergenic, *SNORA48*
3	AGTGA**T**GCAG**CA**TTTCAATA	intergenic, *SNORA18*
3	AGTGAGGC**T**GAC**A**TTCA**G**TA	intron, *ERG*
3	**T**GTGAGGCAGA**A**TTTCA**C**TA	intergenic, *LINC00603*
3	**G**GTG**G**GG**A**AGACTTTCAATA	intergenic, *RP11-460H9.1*
3	AGT**C**AGGCAGA**A**TTTC**G**ATA	intergenic, *RP11-447M12.3*
3	AGTGAGGCAGAC**A**T**C**CAA**A**A	intergenic, *SYT9*
3	AGTGAGGCAG**T**CTT**A**CAA**C**A	intergenic, *SNORD66*
3	AGTGAGGCAGA**T**TTT**T**AAT**C**	intron, *ERC1*
3	A**A**TGAGG**G**AGACTTTCAAT**G**	intron, *FAM154A*
3	A**C**TGAGGCAGACTTTC**C**AT**C**	exon, *CASC2*

3	**T**GTG**G**GGCAG**C**CTTTCAATA	intron, *SNTB1*
3	AGTGAGGCAGACT**C**TCA**CC**A	intergenic, *MBP*
3	AG**A**GAGGCA**A**ACTTTC**C**ATA	intergenic, *RP11-807H17.1*
3	AGTGAGG**A**AGACT**G**T**T**AATA	intergenic, *IL6*
2	AGTGAG**T**CAGACTTTCA**G**TA	intergenic, *VRTN-SYNDIG1*
2	AGTGAGG**A**AGACTTTCAA**A**A	intron, *C6orf211*
1	AGTGAGGCAGA**A**TTTCAATA	intergenic, *ACO11288.2*

Supplementary Table 2. The primer sequences used in this study were the following, related to STAR Methods.

mRNA	*Sense primer*	*Antisense primer*
Pparγ	5'-GCCAGTTTCGATCCGTAGAA-3'	5'-ATTCCTTGGCCCTCTGAGAT-3'
C/ebpα	5'-AAACAACGCAACGTGGAGA-3'	5'-GCGGTCATTGTCACTGGTC-3'
Fasn	5'-TTCCAAGACGAAAATGATGC-3'	5'-AATTGTGGGATCAGGAGAGC-3'
Scd1	5'-CCGGAGACCCCTTAGATCGA-3'	5'-TAGCCTGTAAAAGATTTCTGCAAA-3'
Fabp4	5'-AAGGTGAAGAGCATCATAACCCT-3'	5'-TCACGCCTTTCATAACACATTCC-3'
Wnt10b	5'-GTTAGGTCGAGCAGAGCCAA-3'	5'-TGCTTAGAGCCCGACTGAAC-3'
Ucp-1	5'-ACTGCCACACCTCCAGTCATT-3'	5'-CTTTGCCTCACTCAGGATTGG-3'
Pgc-1α	5'-TATGGAGTGACATAGAGTGTGCT-3'	5'-CCACTTCAATCCACCCAGAAAG-3'
Pgc-1β	5'-AGAAGGTTGGCTGACATGGG-3'	5'-AGGTCAAGCTCTGGCAAGTC-3'
Tnf-α	5'-ATGAGCACAGAAAGCATGATC-3'	5'-TACAGGCTTGTCACTCGAATT-3'
Mcp-1	5'-GCCTGCTGTTCACAGTTGC-3'	5'-CAGGTGAGTGGGGCGTTA-3'
F4/80	5'-TGAATGGCTCCATTTGTGAA-3'	5'-GGCCCTCCTCCACTAGATTC-3'
Hmbs	5'-ATCTTGGACCTAGTGAGTGTGT-3'	5'-GTACAGTTGCCCATCTTTCATCA-3'
Hprt	5'-TCAGTCAACGGGGGACATAA-3'	5'-TGCTTAACCAGGGAAAGCAAA-3'

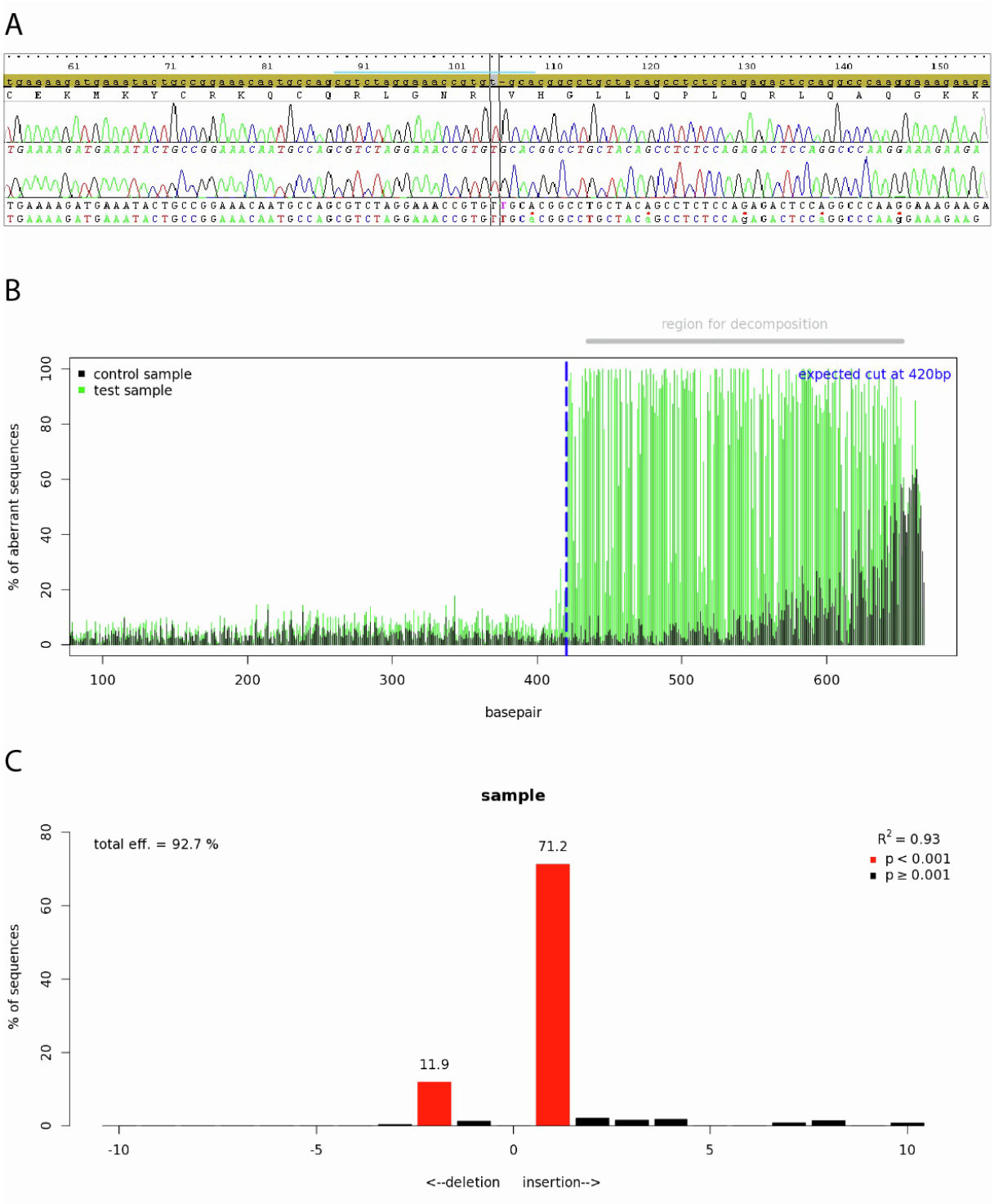

Figure S1. Assessment of CRISPR/Cas9 editing efficiency with gRNA targeting *Mlkl* exon 1 in control and edited 3T3-L1, related to Figure 2. (**A**) Sanger sequencing of the target region (exon 1) confirmed high level of recombination. The gRNA sequence is blue-underlined. (**B**) Determination of CRISPR indel pattern in control and edited ASC by analyzing Sanger sequencing data with the software Tide (https://tide.nki.nl). The discordance plot details the rate of sequence alignment per base between the control and edited samples in the inference window (*i.e.*, the region around the recombination site highlighted by a vertical dotted blue line

and the gRNA sequence is blue-underlined). Before the gRNA target site, the green line (edited sample) and the dark-green line (control sample) are close together. After the gRNA target site, a jump is observed, corresponding to a high level of sequence misalignment. (**C**) The graph displays the frequency of indels in relationship with the indel size. The editing efficiency corresponding to the recombination rate was evaluated at 93%.

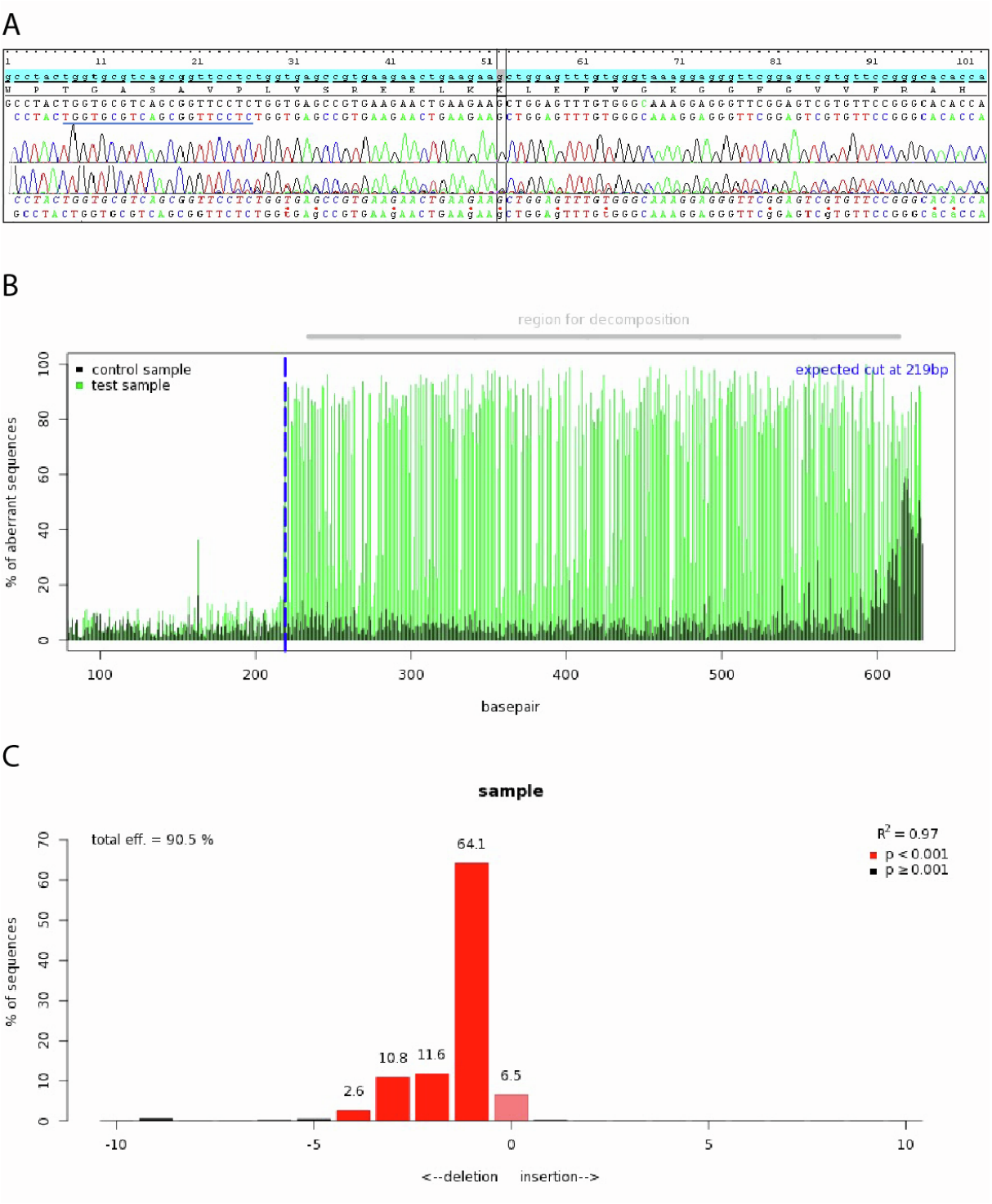

Figure S2. Assessment of CRISPR/Cas9 editing efficiency with gRNA targeting *Ripk3* exon 1 in control and edited 3T3-L1, related to Figure 2. (**A**) Sanger sequencing of the target region (exon 1) confirmed high level of recombination. The gRNA sequence is blue-underlined. (**B**) Determination of CRISPR indel pattern in control and edited ASC by analyzing Sanger sequencing data with the software Tide (https://tide.nki.nl). The discordance plot details the rate of sequence alignment per base between the control and edited samples in the inference window (*i.e.*, the region around the recombination site highlighted by a vertical dotted blue line

and the gRNA sequence is blue-underlined). Before the gRNA target site, the green line (edited sample) and the dark-green line (control sample) are close together. After the gRNA target site, a jump is observed, corresponding to a high level of sequence misalignment. (**C**) The graph displays the frequency of indels in relationship with the indel size. The editing efficiency corresponding to the recombination rate was evaluated at 91%.

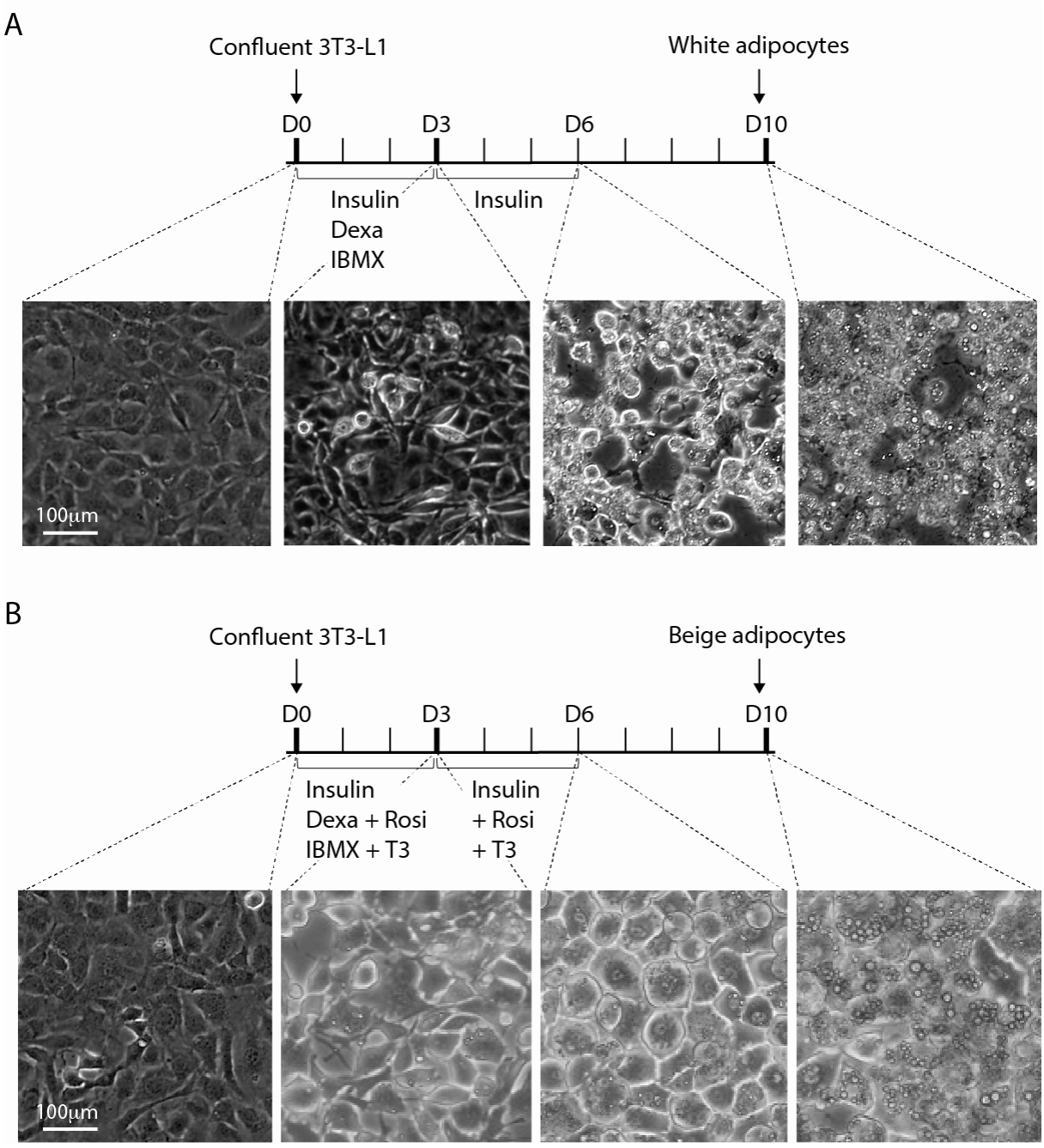

Figure S3. Timeline representation of the 3T3-L1 pre-adipocyte differentiation process using hormonal cocktails, related to Figure 3. (**A**) Protocol for white adipocyte differentiation. (**B**) Protocol for beige adipocyte differentiation. Dexa: dexamethasone; IBMX: 3-isobutyl-1-methylxanthine; Rosi: rosiglitazone; T3: triiodothyronine; D0–D10: Day 0 to Day 10.

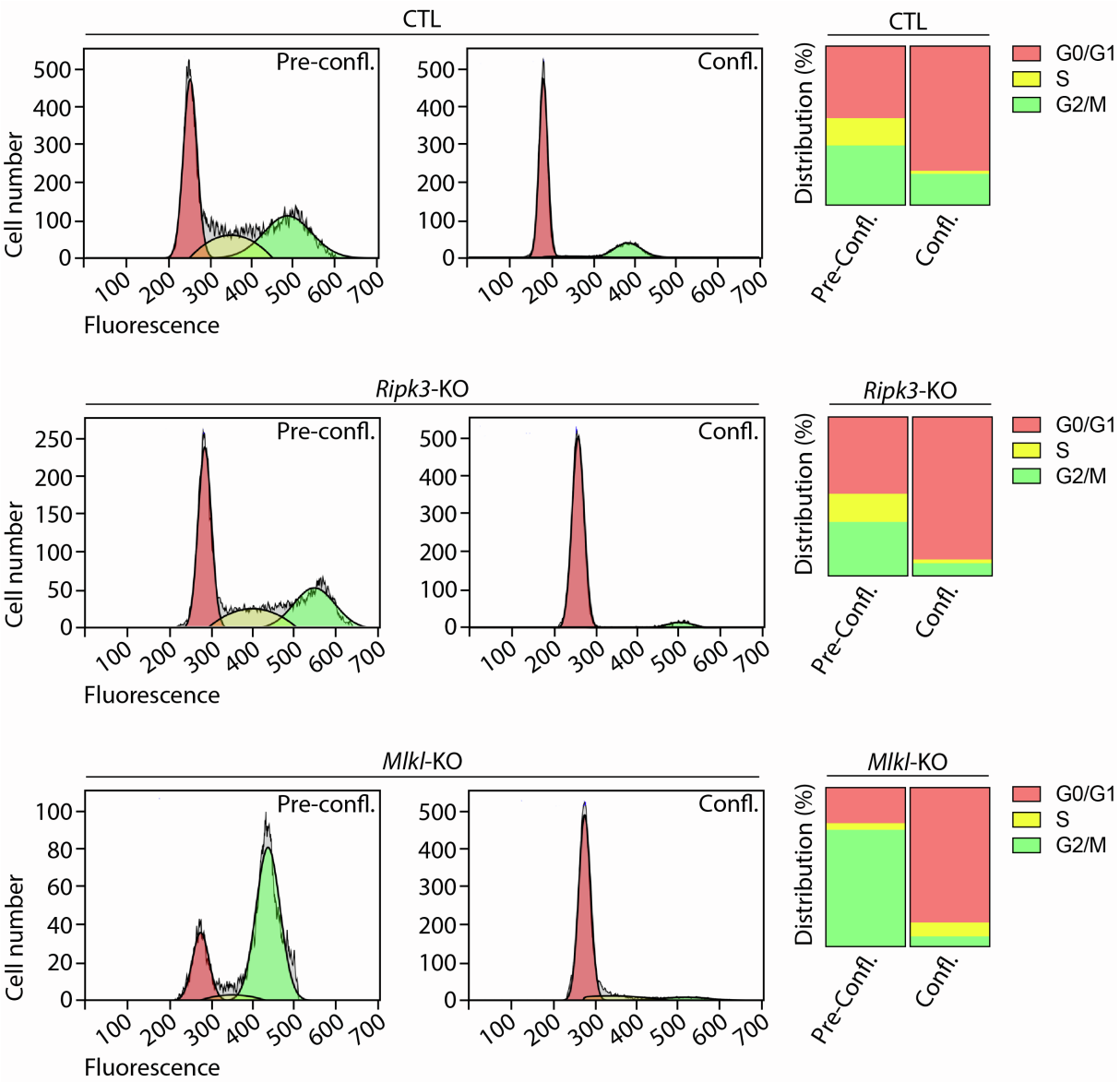

Figure S4. Cell cycle arrest analysis of the 3T3-L1 cells, related to Figure 3. Data were obtained in 3T3-L1 with a CRISPR-Cas9-mediated *Ripk3*- or *Mlkl*-knockout (KO), and 3T3-L1 transduced with a Cas9/scramble gRNA plasmid corresponding to control (CTL) cells. Flow cytometry using PI staining was used to determine the cell cycle distribution of pre-confluent and confluent 3T3-L1 cells. Pre-Confl.: pre-confluence; Confl.: confluence.

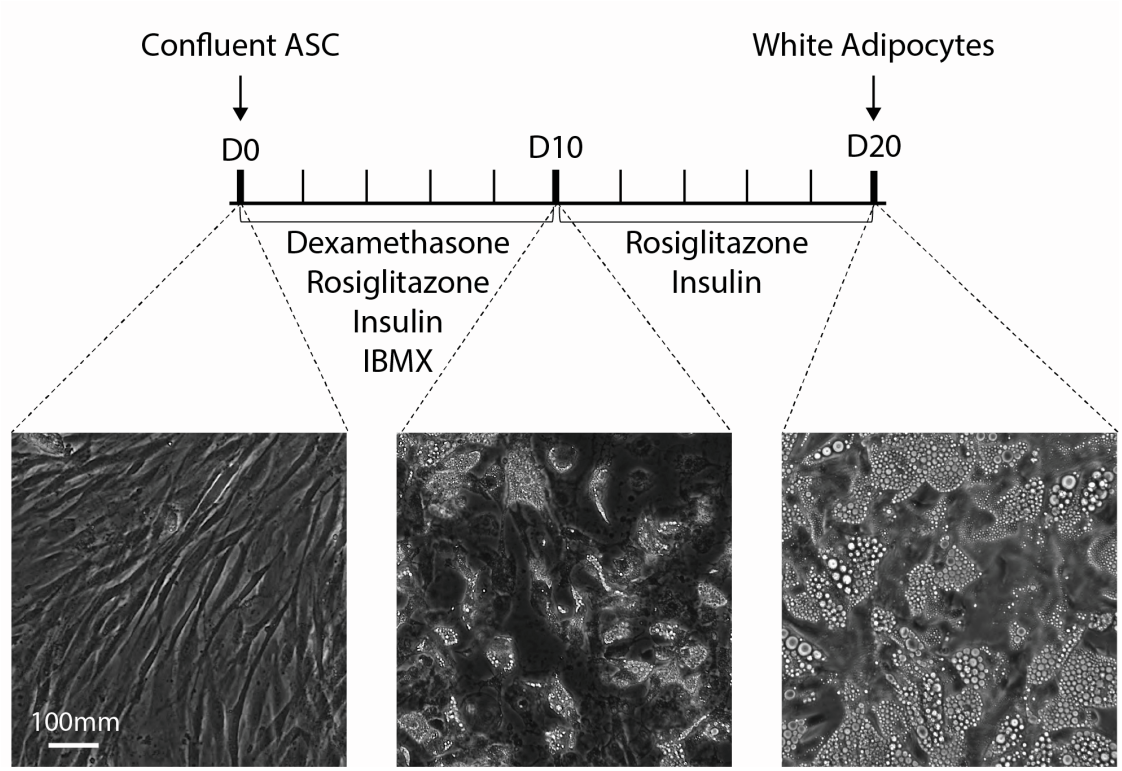

Figure S5. Timeline representation of the ASC differentiation process into white adipocytes using a hormonal cocktail, related to Figure 3. ASC, human adipose stem cell; IBMX: 3-isobutyl-1-methylxanthine; D0: day 0; D10: day 10; D20: day 20.

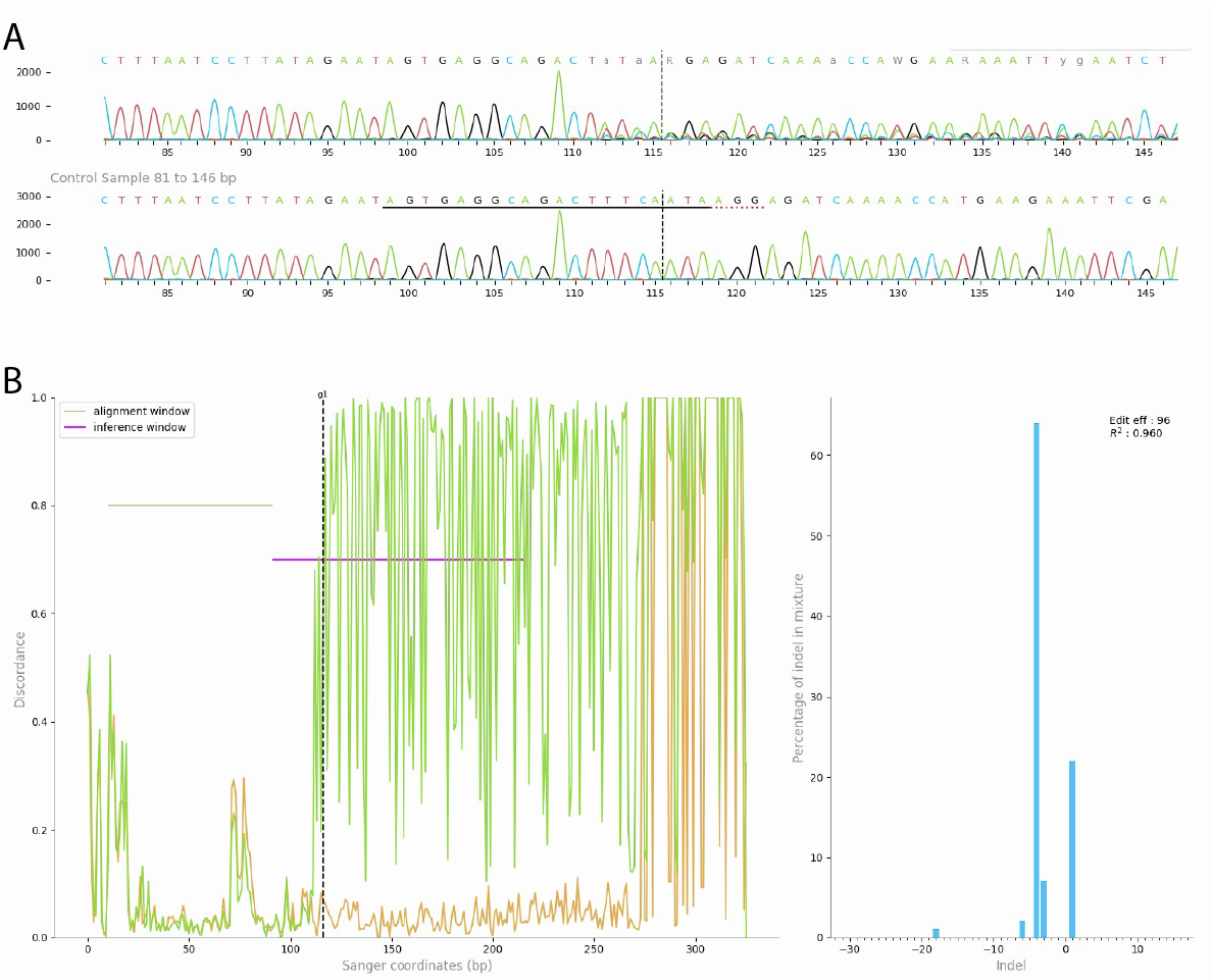

Figure S6. Assessment of CRISPR/Cas9 editing efficiency with gRNA targeting *MLKL* exon 1 in control and edited ASC, related to Figure 3. (**A**) Sanger sequencing of the target region (exon 4) confirmed high level of recombination. The expected break site is indicated by a vertical dotted line and the gRNA sequence is underlined. (**B**) Determination of CRISPR indel pattern in control and edited ASC by analyzing Sanger sequencing data with the Synthego software (https://ice.synthego.com). Left panel: The discordance plot details the rate of sequence alignment per base between the control and edited samples in the inference window (i.e., the region around the recombination site). Before the gRNA target site, the green line (edited sample) and the orange line (control sample) are close together. After the gRNA target site, a jump is observed, corresponding to a high level of sequence misalignment. Right panel: The graph displays the frequency of indels in relationship with the indel size. The editing efficiency corresponding to the recombination rate was evaluated at 96%.

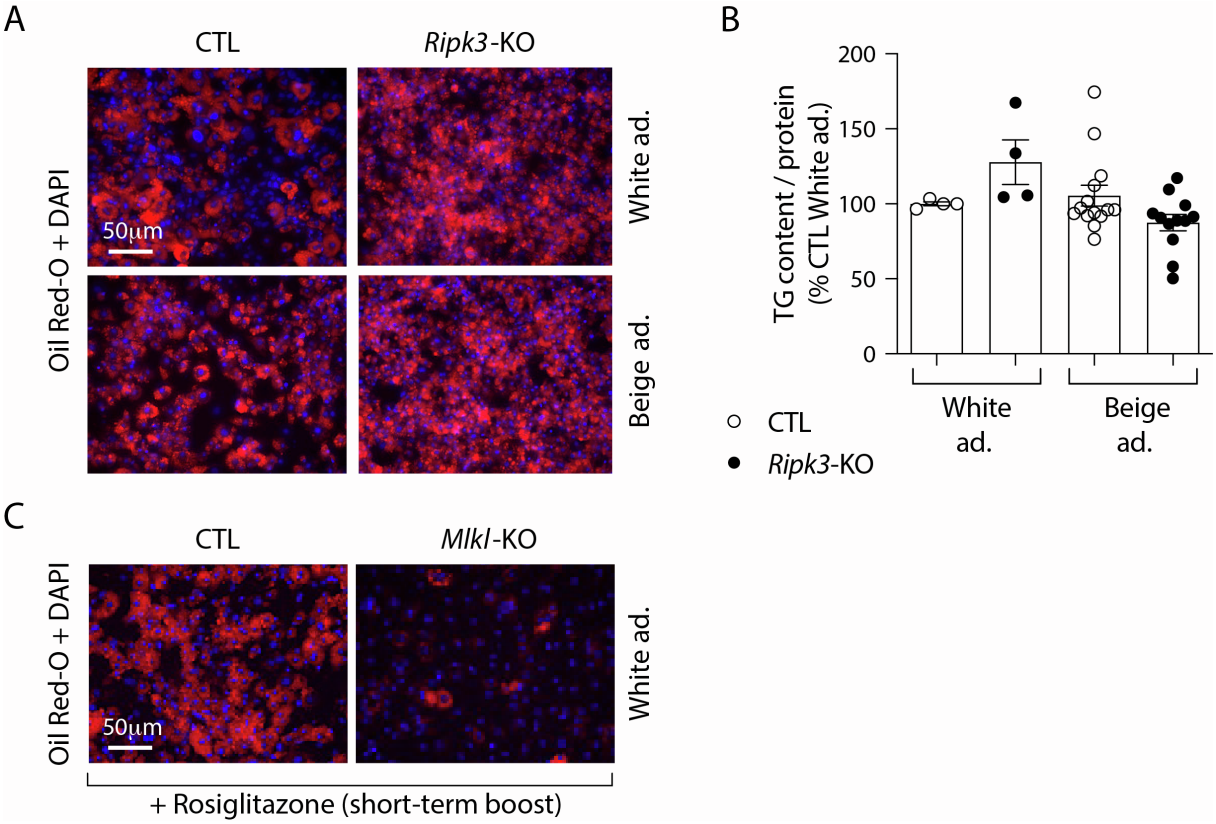

Figure S7. *Ripk3* deficiency does not alter the differentiation of 3T3-L1 into beige adipocytes, related to Figure 4. Data were obtained in 3T3-L1 with a CRISPR-Cas9-mediated *Ripk3*- or *Mlkl*-knockout (KO), and 3T3-L1 transduced with a Cas9/scramble gRNA plasmid corresponding to control (CTL) cells. (**A**) 3T3-L1 adipocytes were assessed by Oil Red O (Red) and nuclei (DAPI, blue) at the final stage of differentiation (D10). Images are representative of three independent experiments. (**B**) Quantification of Oil Red O fluorescence normalized to DNA content (DAPI). Results are expressed as means ± SEM of three independent experiments. (**C**) CTL and *Mlkl*-KO 3T3-L1 cells were differentiated into white adipocytes using a short-term boost of rosiglitazone between D0-D3 of the differentiation protocol (please also refer to the Supplementary Figure 4A).

A

Sample name	Raw reads	Clean reads	Raw bases	Clean bases	Error rate(%)	Q20(%)	Q30(%)	GC content(%)
J0CTL1	42894509	42296200	12.9G	12.7G	0.02	97.97	94.37	50.74
J0CTL2	35634301	35068030	10.7G	10.5G	0.02	98.02	94.55	50.66
J0CTL3	30351630	29871056	9.1G	9.0G	0.03	97.88	94.21	50.82
J0RIPK31	31680446	31069225	9.5G	9.3G	0.02	98.05	94.58	50.89
J0RIPK32	28616103	28107144	8.6G	8.4G	0.02	97.99	94.43	50.79
J0RIPK33	46400698	45585557	13.9G	13.7G	0.03	97.87	94.18	51.01
J0MLKL1	29147301	28703216	8.7G	8.6G	0.02	98.01	94.46	50.73
J0MLKL2	36941244	36472122	11.1G	10.9G	0.02	98.02	94.45	50.96
J0MLKL3	32426267	31966606	9.7G	9.6G	0.02	98.01	94.45	50.57
J7CTL1	31221019	30774344	9.4G	9.2G	0.02	98.02	94.50	50.98
J7CTL2	31429372	30980615	9.4G	9.3G	0.02	98.06	94.59	50.74
J7CTL3	34607850	34097681	10.4G	10.2G	0.02	98.01	94.50	50.73
J7RIPK31	31709735	31223444	9.5G	9.4G	0.02	97.96	94.34	50.79
J7RIPK32	26310118	25956449	7.9G	7.8G	0.03	97.75	93.64	50.74
J7RIPK33	33960992	33408511	10.2G	10.0G	0.03	97.78	93.72	50.52
J7MLKL1	32914150	32245436	9.9G	9.7G	0.02	98.03	94.52	50.36
J7MLKL2	27562379	26950424	8.3G	8.1G	0.02	98.04	94.52	50.14
J7MLKL3	35521747	34685265	10.7G	10.4G	0.02	97.96	94.41	50.34

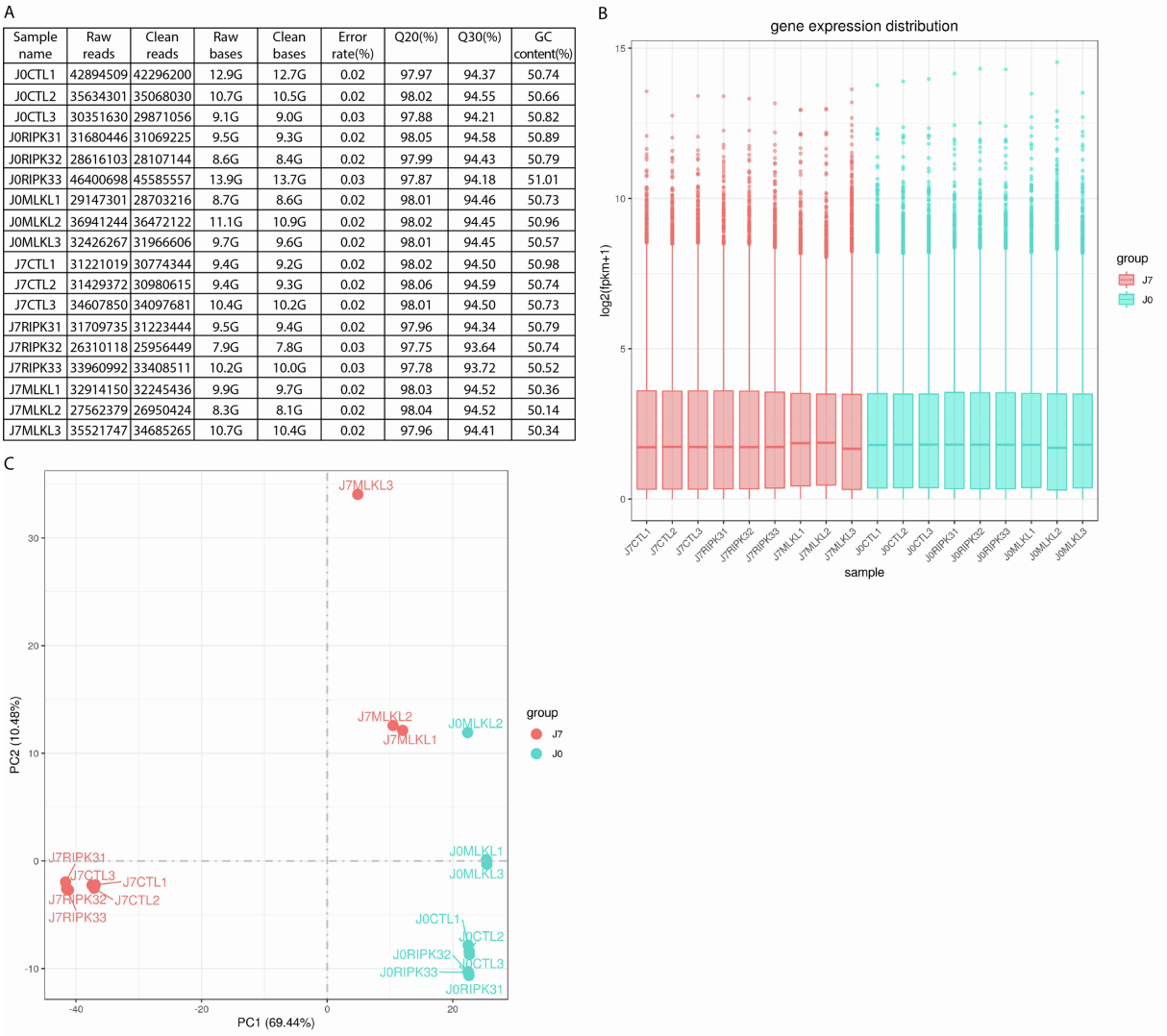

Figure S8. RNA sequencing quality control and reads processing, related to Figure 5. (**A**) QC stats and number of clean reads for each replicate before alignment. (**B**) Gene expression distribution across samples (**C**) Principal component analysis in between replicates. J0 means Day 0 (basal stage) and J7 Day 7 (differentiated cells).

A

D0 *Mlkl*-KO *vs.* D0 CTL (GO)

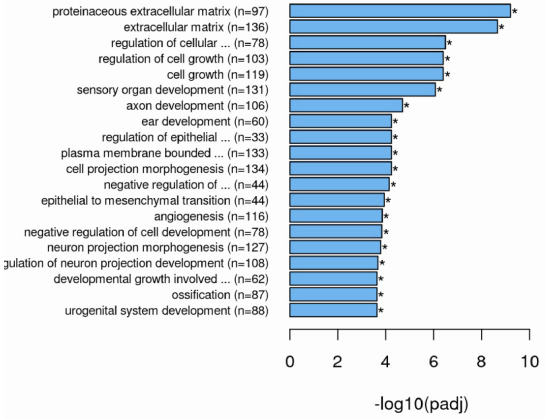

B

GO 0001503: Ossification

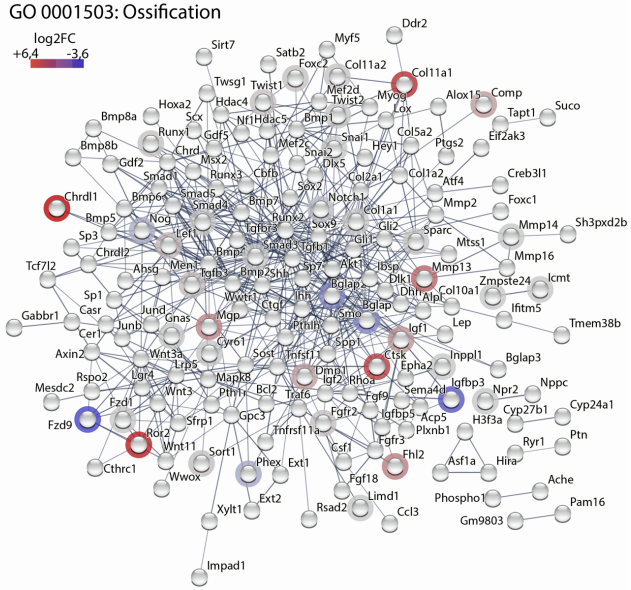

C

D0 *Ripk3*-KO *vs.* D0 CTL (GO)

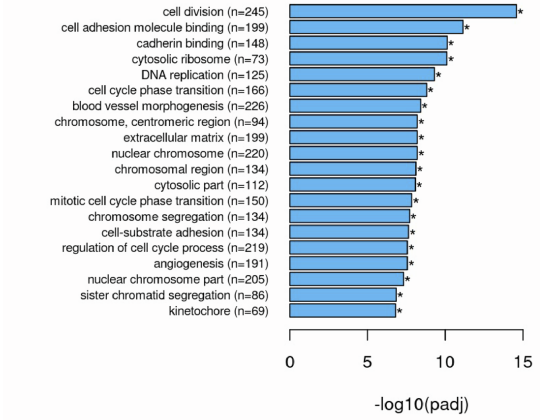

D

WikiPathways WP413: G1 to S cell cycle control

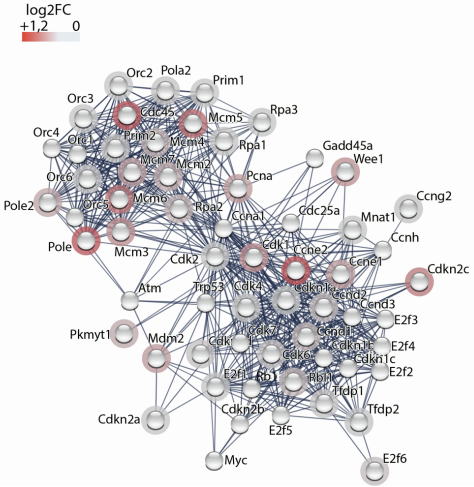

Figure S9. Differential expressed genes enrichment analysis before differentiation, related to Figure 5. (**A**) Gene ontology analysis for significantly changed DEGs in *Mlkl*-KO vs CTL cells at D0. (**B**) Protein interaction network in *Mlkl*-KO vs CTL cells for GO 0001503: Ossification generated using STRING-db. (**C**) Gene ontology analysis for significantly changed DEGs in *Ripk3*-KO vs CTL cells at D0. (**D**) Protein interaction network in *Ripk3*-KO vs CTL cells for WP413: G1 to S cell cycle control using STRING-db.

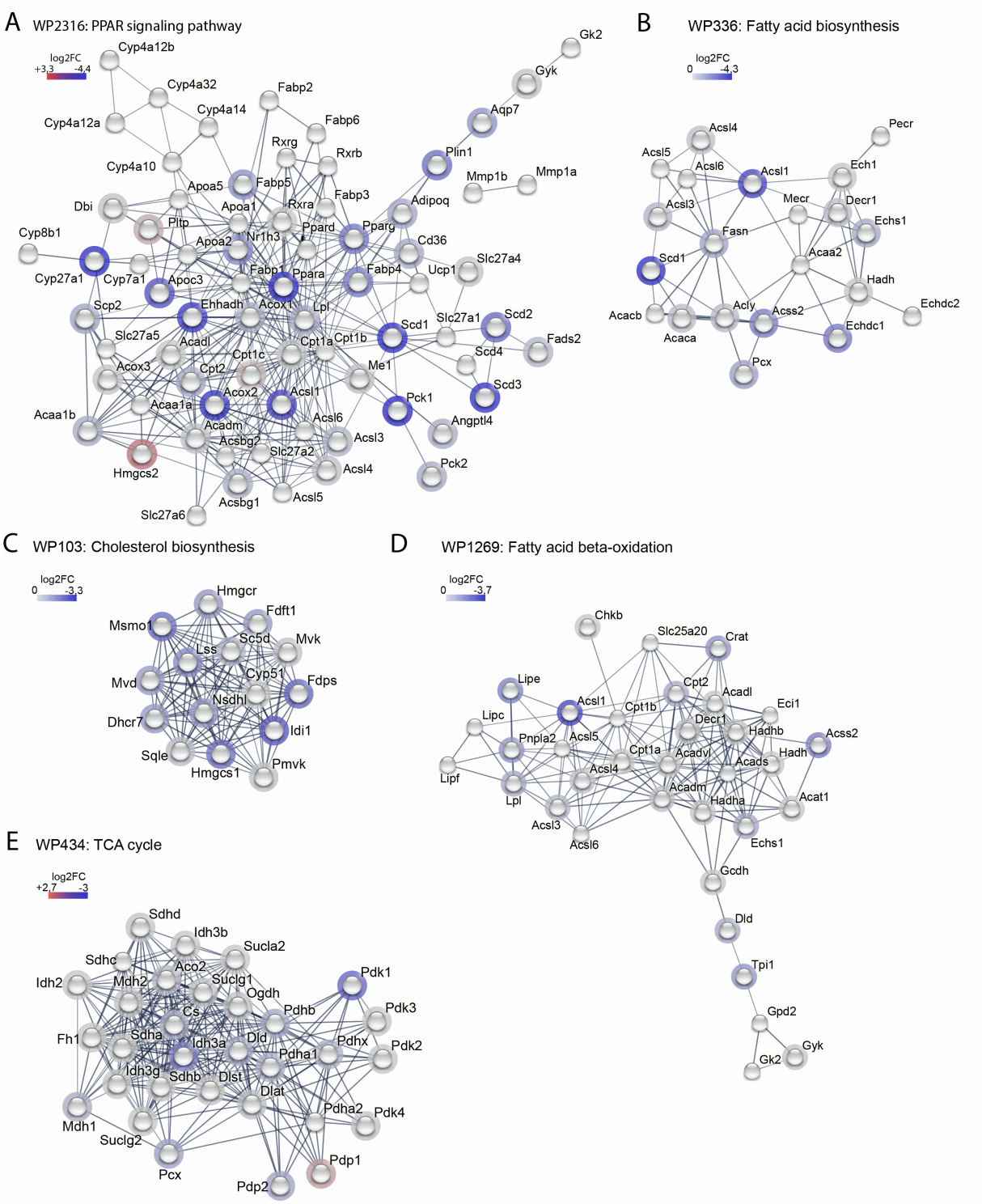

Figure S10. Interaction networks in *Mlkl*-KO cells *vs.* CTL cells 7 days post-differentiation, related to Figure 5. All networks were generated using STRING-db protein interaction network for WP2316: PPAR signaling pathway (**A**); WP336: Fatty acid biosynthesis (**B**); WP103: Cholesterol biosynthesis (**C**); WP1269: Fatty acid beta-oxidation (**D**); WP434: TCA cycle (**E**).

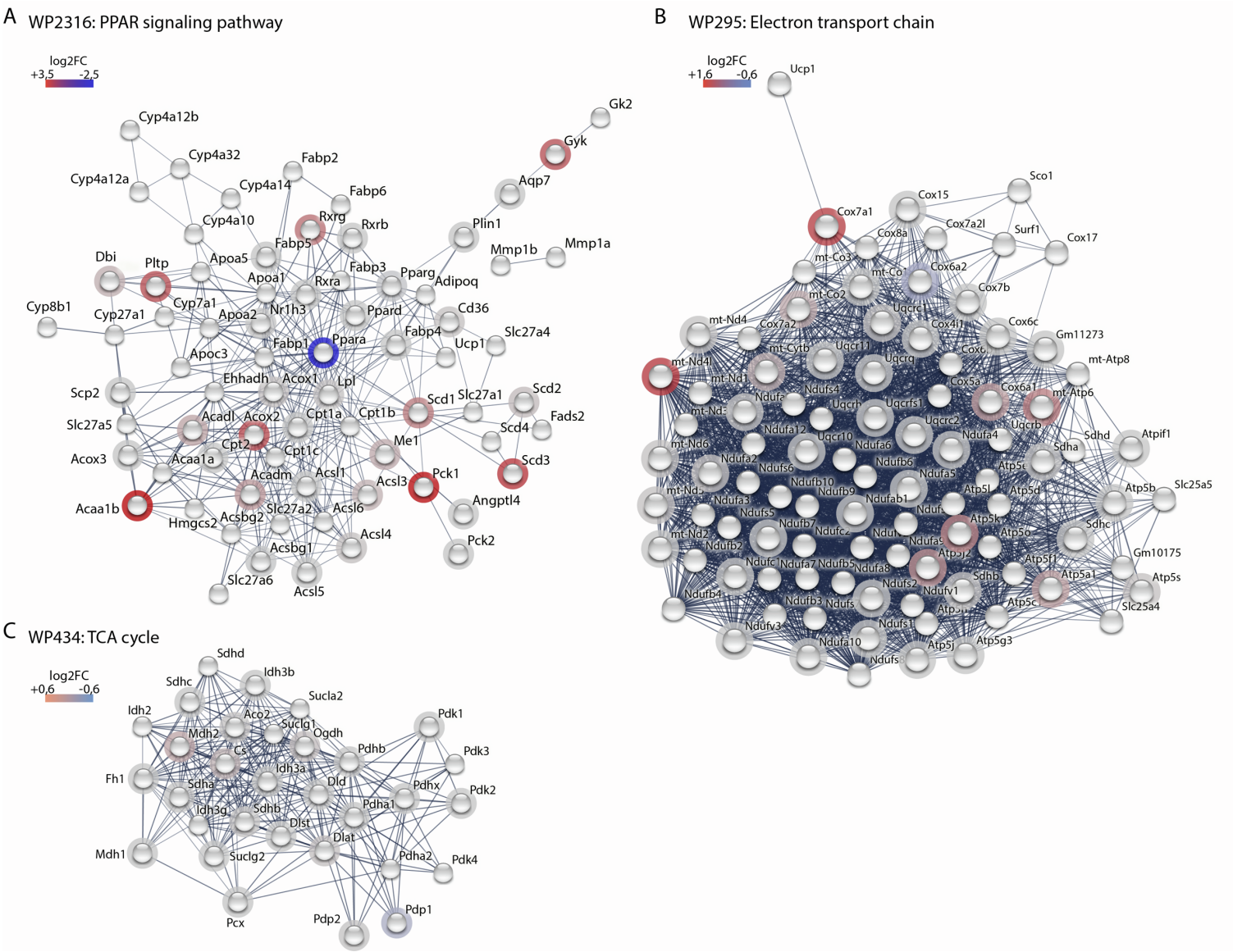
A
WP2316: PPAR signaling pathway
log2FC
+3,5 -2,5
Cyp4a12b
Cyp4a32
Cyp4a12a
Cyp4a14
Cyp4a10
Fabp2
Fabp6
Rxrg
Rxrb
Fabp5
Fabp3
Pparg
Adipoq
Gk2
Gyk
Aqp7
Plin1
Mmp1b
Mmp1a
Dbi
Pltp
Apoa5
Apoa1
Rxra
Cyp8b1
Cyp27a1
Cyp7a1
Apoa2
Nr1h3
Ppard
Cd36
Fabp1
Ppara
Fabp4
Ucp1
Slc27a4
Apoc3
Ehhadh
Acox1
Lpl
Scp2
Acadl
Acox2
Cpt1a
Cpt1b
Scd1
Slc27a1
Scd2
Fads2
Slc27a5
Cpt2
Cpt1c
Me1
Scd4
Acox3
Acaa1a
Acadm
Acsl1
Acsl3
Pck1
Scd3
Acaa1b
Slc27a2
Acsl6
Angptl4
Hmgcs2
Acsbg2
Acsl4
Pck2
Acsbg1
Slc27a6
Acsl5
B
WP295: Electron transport chain
log2FC
+1,6 -0,6
Ucp1
Cox7a1
Sco1
Cox15
Cox7a2l
Surf1
Cox17
Cox8a
mt-Co3
mt-Co1
Cox6a2
Cox7b
mt-Co2
Uqcrc1
Cox4i1
Cox6c
mt-Nd4
Cox7a2
Gm11273
mt-Cytb
Uqcr11
Uqcrq
Cox6b
mt-Atp8
mt-Nd4l
mt-Nd1
Cox5a
Cox6a1
mt-Atp6
Ndufs4
Uqcrh
Uqcrfs1
Uqcrc2
Ndufa12
Uqcr10
Ndufa6
Ndufa4
Uqcrb
Sdhd
Atpif1
Sdha
mt-Nd6
Ndufa2
Ndufs6
Ndufb6
Ndufa5
Atp5c
Ndufb10
Ndufb9
Ndufab1
Atp5l
Atp5d
Atp5b
Slc25a5
Ndufa3
Ndufs5
Ndufb7
Ndufc2
Atp5k
Atp5o
Sdhc
mt-Nd2
Ndufb2
Ndufa8
Gm10175
Ndufc
Ndufa7
Ndufb5
Atp5f1
Atp5a1
Atp5s
Sdhb
Ndufs2
Ndufv1
Ndufb4
Ndufb3
Ndufs
Atp5c
Slc25a4
Ndufv3
Ndufs1
Ndufa10
Atp5j
Atp5g3
Ndufs
C
WP434: TCA cycle
log2FC
+0,6 -0,6
Sdhd
Idh3b
Sdhc
Sucla2
Idh2
Aco2
Pdk1
Suclg1
Mdh2
Ogdh
Pdhb
Pdk3
Cs
Idh3a
Fh1
Dld
Pdhx
Pdk2
Sdha
Pdha1
Idh3g
Sdhb
Dlst
Dlat
Mdh1
Suclg2
Pdha2
Pdk4
Pcx
Pdp2
Pdp1

Figure S11. Interaction networks in *Ripk3*-KO cells *vs.* CTL cells 7 days post-differentiation, related to Figure 5. All networks were generated using STRING-db: WP2316: PPAR signaling pathway (**A**); WP295: Electron transport chain (**B**); WP434: TCA cycle (**C**).

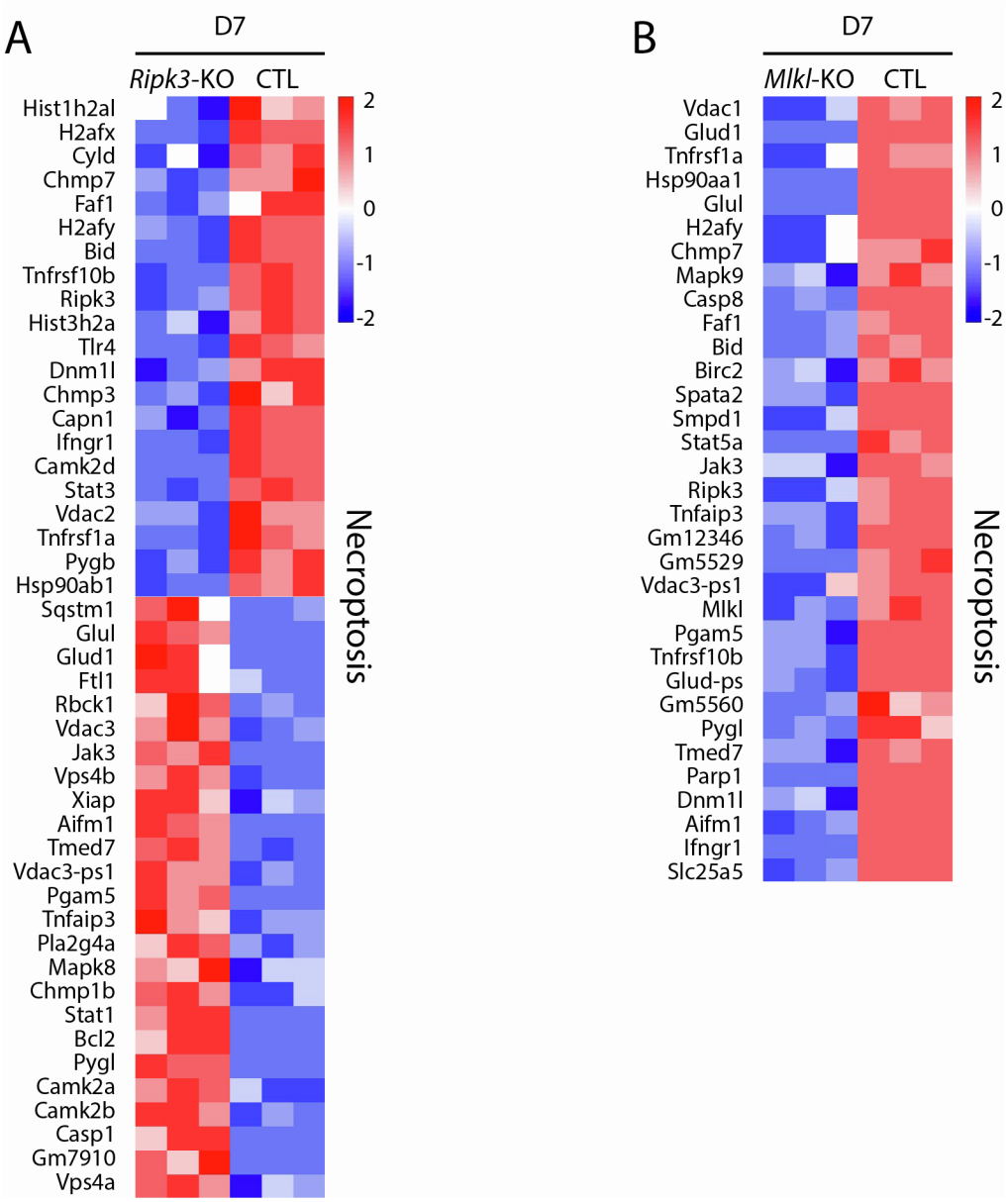

Figure S12. Differentially expressed gene clustered for necroptosis pathway, related to Figure 5. Hierarchical clustering heatmap of fragments per kilobase million (FPKM) values of differentially expressed genes in differentiated 3T3-L1 cells (Day 7) between CTL and *Ripk3*- (**A**) or *Mlkl*- (**B**) deficient cells. Red represents high FPKM values and blue represents low FPKM values. Color descending from red to blue indicates log 10 (FPKM + 2) from high to low expression.

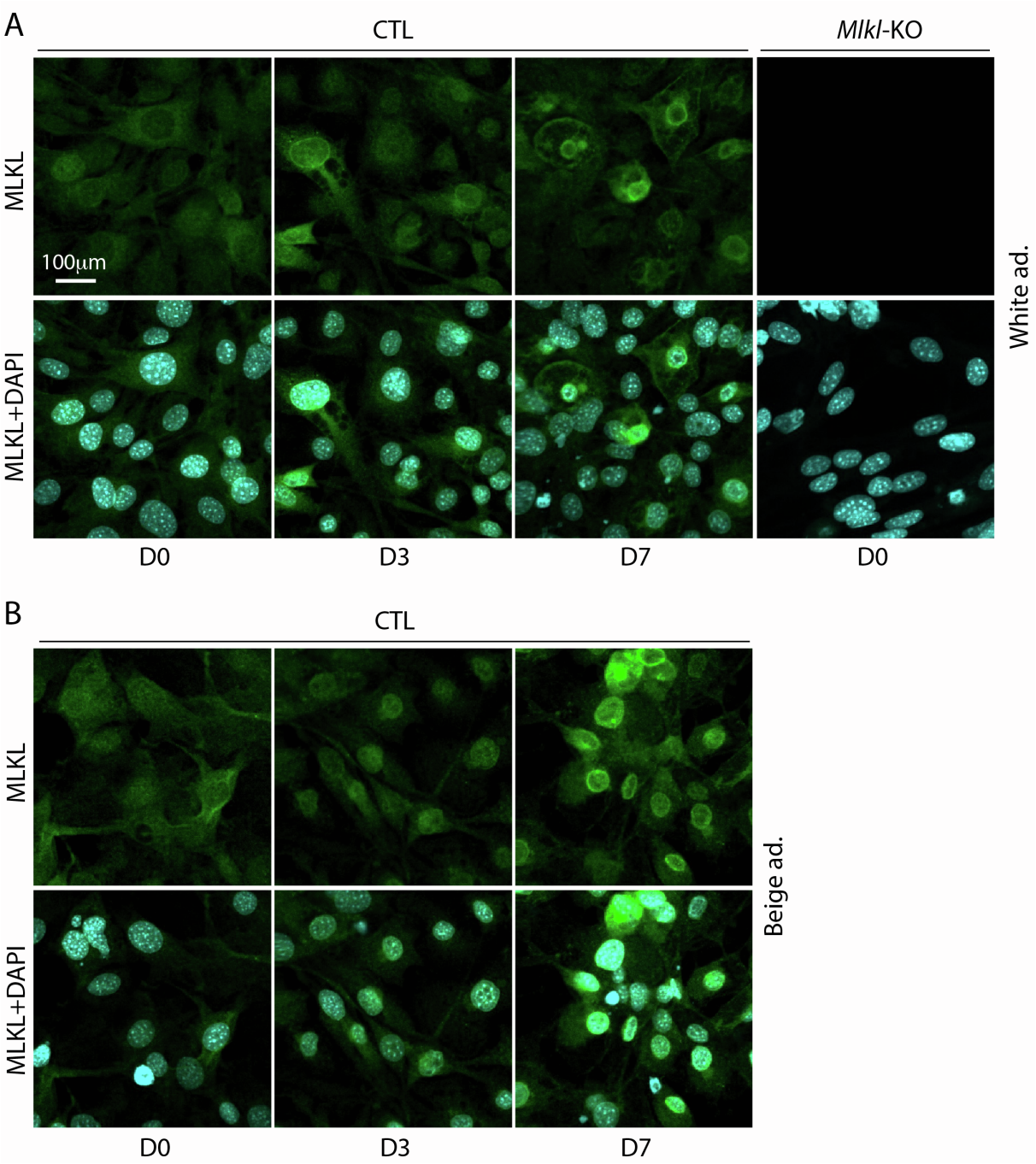

Figure S13. MLKL is located in both cytoplasm and nucleus in adipocytes, related to Figure 4. Confocal microscopy was used to detect endogenous MLKL in control (CTL) 3T3-L1 cells by immunostaining with anti-MLKL antibody. *Mlkl*-KO cells were also stained as a negative control. The nuclei were counterstained with DAPI. The 3T3-L1 cells were differentiated into either white (**A**) or beige (**B**) adipocytes. D0-D7: Day 0 to Day 7.